

**International Journal of Biology, Pharmacy
and Allied Sciences (IJBPAS)**

'A Bridge Between Laboratory and Reader'

www.ijbpas.com

**FABRICATION AND CHARACTERIZATION OF ELECTROSPUNNED
PENTOXIFYLLINE LOADED BIOCOMPATIBLE PVA: PVP BASED
NANOFIBROUS MUCOADHESIVE FILM FOR THE ORAL SUBMUCOUS
FIBROSIS**

NETKE S¹, PAWAR A¹, JADHAV P² AND MALI A^{1*}

1: Department of Pharmaceutics, Poona College of Pharmacy, Bharati Vidyapeeth (Deemed to be University), Pune 38, Maharashtra, India

2: Department of Pharmaceutics, Yashoda college of pharmacy, Satara, Maharashtra, India

***Corresponding Author: Dr. Ashwin J Mali: E Mail: ashwinjmali@rediffmail.com**

Received 18th July 2023; Revised 20th Sept. 2023; Accepted 2nd Dec. 2023; Available online 1st Sept. 2024

<https://doi.org/10.31032/IJBPAS/2024/13.9.8309>

ABSTRACT

Nanofiber (NF) represents one of the newest, promising and advanced technologies in transdermal and oromucosal drug delivery due to its unique advantages. The present study aims to fabrication of electrospun pentoxifylline loaded biocompatible PVA: PVP based nanofibrous mucoadhesive film for the oral submucous fibrosis. The fabricated NF film mechanical and physicochemical properties were assessed. These nanofibers were then characterised for drug content, FTIR, DSC, SEM), XRD analysis, in-vitro diffusion and ex-vivo permeation studies using franz diffusion cells. The SEM and IR elucidated the thin, uniform, smooth surface of NF without bead formation and interaction between drug and polymers. The PXRD and DSC revealed the molecular dispersion with less crystalline nature of the NF. The diffusion and permeation study resulted initial burst release with gradual diffusion with zero order kinetics. Using the electrospinning approach, PTX-loaded nanofiber film was successfully fabricated and can be explored as biocompatible film for the effective cure of oral Submucous Fibrosis.

Keywords: Nanofiber, Electrospinning, Pentoxifylline, Oral Submucous Fibrosis

INTRODUCTION

Oral submucous fibrosis (OSMF) is a persistent, intricate and precancerous disorder with a high risk. The patient with OSMF has the typical inflammation in the juxta-epithelial cells with excessive collagen formation (progressive fibrosis) of the submucosal tissues (*lamina propria* and deeper connective tissues) [1]. It is a potentially cancerous condition that is most common among people of asian heritage. The oral cavity, pharynx and upper portion of the esophagus are the primary sites of OSMF induced by chronic consumption of areca nut and commercial preparations [2]. In this condition, mucosal stiffness of oral mucosa is the prominent early sign which further sporadically transfer to the pharynx and esophagus region which results in locking of jaws and further has a potential risk of malignant transformation [3-6]. As per the statistics, the prevalence of OSMF in India stands between 0.2 to 2.3% mehortility affecting male population from South and South East Asia [7] and which can be attributed to the rising popularity of chewing pan masala (areca nut) among younger generations [8, 9]. Further, the consumption of commercialized smokeless tobacco products, a high intake of chilies in the diet, the presence of dangerous traces of copper in

food products, micronutrient deficiencies and genetic predisposition are some additional risk factors that have been hypothesized to contribute to the disease process [10].

Pentoxifylline (PTX), is a xanthine derivative, has a wide range of biological functions such as anti-inflammatory, antioxidant and vasodilator properties which preferred to treat muscle pain in people with peripheral artery disease [11]. It reduces collagen synthesis, interleukin-6 expression and transforming growth factor-beta1 expression in hepatic stellate [12-15]. PTX is a water-soluble with a LogP value of 0.3. It undergoes extensive first-pass metabolism resulting in its poor bioavailability (20 %) and short half-life (0.4–0.8 h) [16, 17]. Further, PTX has most prevalent adverse effects like nausea and vomiting, dyspepsia, bloating, flatus, headache, dizziness, tremor, anxiety and disorientation [18]. Therefore, there is a need to draw a fine line between therapeutic and toxic concentration of PTX by developing the novel drug delivery with controlled site specific release of PTX which help to maintain the optimum concentration of PTX at a particular site of infection.

The development of novel carrier that can deliver PTX to the target site of action in a controlled manner is a viable means of

lowering the frequency of systemic exposure and unfavourable side effects with establishment of standard and safe line of treatment [19]. One such delivery technology such like nanofibers (NFs) is useful for treating many diseases because of their unique features like large surface area and highly adaptable architectures [20-24]. Further, NFs are advantageous because they may administer medications through transdermal, oral, sustained, depot and other routes [25-27]. Additionally, dependent on their technique of manufacture, electrospun nanofibers provide a regulated release profiles including delayed, pulsatile and rapid biphasic release of bioactive [28]. Electrospinning is regarded as a flexible technique for producing continuous polymeric nanofibrous material due to its efficiency among the several described approaches [29-34].

The present study deals with the development and evaluation of the poly vinyl alcohol (PVA): polyvinyl pyrrolidone (PVP) based nanofibrous oral film containing PTX. The PVA is a ridged polymer that has a lower oral solubility and mucoadhesion capability when used alone. To overcome this, mucoadhesive pore-forming (highly soluble) polymer is therefore required to work with PVA. The polyvinyl pyrrolidone

(PVP) is a more soluble and mucoadhesive polymer to meet this demand due to its target specific activity. To achieve nanofibers (NF) with the smallest diameter and most drug entrapment capacity, many of the process primary independent variables including the PVA: PVP ratio, the rate of the electro-spinner jet and the distance between the electro-spinning needle and collector were tuned. These nanofibers were then characterised for drug content, Fourier transform infrared spectroscopy (FTIR), Differential scanning calorimetry (DSC), Scanning electron microscopy (SEM), X-ray diffraction (XRD) analysis (XRD), in-vitro diffusion and ex-vivo permeation studies using franz diffusion cells.

MATERIALS AND METHOD

Materials

Pentoxifylline (PTX) is supplied by Supriya Life science Ltd, Ratnagiri as a kind gesture. Polyvinyl alcohol (PVA) and polyvinyl pyrrolidone K-300 (PVP) was purchased from Loba Chemie Pvt Ltd Mumbai, India. All other solvents used in the study were purchased from Merck Ltd, Mumbai, India.

Method

Preparation of Spinning Solution

The 5% of PVP dissolved in deionised (DI) water with warm heating with constant stirring. Then equal amount of PVA was

added into the previous solution with frequent heating as well as constant stirring. After dissolving the polymers, PTX (0.5%) is added to the previous solution at room temperature with constant stirring of 200 rpm for 4 h.

Preparation of Nanofibers

The prepared solutions were inserted using a 22-gauge needle into a 5 mL syringe. Using a syringe pump, the feeding rate (0.2 mL/h) was managed. The metallic needle received an 18 kV high voltage feed. The ultrafine fibres were collected using a piece of aluminium foil held 15 cm away from the needle tip using E-Spin Nano (PECO-Chennai, India). For comparison, PTX-loaded PVP/PVA films were also created using the solvent casting approach with solutions of similar composition.

Characterization

Entrapment efficiency (EE)

Quantification of PTX loaded into PVP/PVA nanofibres and solvent cast film was done using a UV spectrophotometric technique. In a short, 10 mL of 6.8 pH phosphate buffer was used to dissolve the PTX-loaded e-spun PVP/PVA fibre and cast PTX loaded film (cut into 2×2 cm in dimension). To determine the precise amount of PTX in each solution, the absorbance was measured at 272 nm using a UV spectrophotometer (Shimadzu

UV1900i). The results of the drug content analysis were utilised to calculate the EE using Equation [35].

$$\%EE = \frac{\text{Weight of Pentoxifylline in Nanofiber mat or film}}{\text{Total weight of Pentoxifylline loaded}} \times 100$$

Scanning Electron Microscopy

The morphology of PTX loaded e-spun PVP/PVA fiber film as well as solvent cast film was characterized using SEM (JEOL JSM-6360A, Tokyo, Japan). The fiber film was mounted on an aluminium stud and coated with a thin layer of platinum using an auto fine coater before observation (Joel, JFC, Tokyo, Japan). The average diameter of PTX loaded e-spun film was measured.

Differential Scanning Calorimetry

A thermal behaviour of PTX, e-spun PVA/PVP film and PTX loaded nanofiber film was examined using DSC in a calorimeter equipped with an intra-cooler (Mettler-Toledo, Greifensee, Switzerland). Indium standards were used to calibrate the temperature and enthalpy scale. Approximately 5 mg of sample was hermetically sealed in an aluminium pan with a hole and heated at a constant rate of 10 °C /min over a temperature range of 50-350 °C. Inert atmosphere was maintained by purging nitrogen gas at a flow rate of 50 mL/min [36].

Powder x-ray diffraction

The x-ray diffractometer was used to perform wide-angle XRD studies of PTX alone, PTX loaded nanofibre film, and PTX loaded as cast film (RigaKu, Tokyo, Japan). This detects crystal lattice and is a powerful tool for studying polymorphism, salts and crystalline phases. The PXRD was recorded on sample exposed to nickel filtrate radiation (40 KV, 30 mA) and were scanned from 10-40 °C with 2θ at a size of 0.045 degree and step time of 0.5 s.

Fourier transforms infrared spectroscopy

The FTIR (FT/IR4100, JASCO International Co., Ltd., Tokyo, Japan) was used to analyse the PTX alone, blank PVA/PVP nanofibres, PTX loaded nanofiber film and PTX loaded as cast films. In order to fill the mould, the samples were combined with dry potassium bromide (2 mg sample in 200 mg KBr). The samples IR spectra were captured in the range of 4000 to 400 cm^{-1} .

In-vitro drug diffusion studies

Franz diffusion cell (Dolphin Instruments, Mumbai, India) with a 32 mL reservoir capacity was used for *in vitro* drug diffusion investigations on dry PTX loaded nanofiber and casted film samples. Each sample, which contained 50 mg of PTX, was cut into squares measuring 2 x 2 cm. Over the cellophane membrane, the disc was positioned in a donor compartment and

parafilm. The phosphate buffer pH 6.8 containing receptor compartment's temperature was held constant at 37 °C throughout the experiment. By removing 1 mL of buffer from the receptor compartment at specified intervals and replacing it with an equal volume of buffer, sink conditions were maintained throughout the experiment and the quantity of PTX that diffused across the membrane was calculated. The samples were filtered using Whatman filter paper and their PTX concentration was determined spectrophotometrically at a wavelength of 272 nm.

Ex-vivo skin permeation studies

PTX loaded nanofiber and casted film samples were studied for *ex-vivo* skin penetration utilizing franz diffusion cells equipped with pig mucosal skin [37]. We used a vertical franz diffusion cell with a 32 mL reservoir and a surface area of 2.54 cm^2 . Throughout the experiment, phosphate buffer pH 6.8 was continuously stirred using a magnetic stirrer in the receptor compartment. The buffer temperature was maintained constant at 37°C. The PTX-loaded nanofiber and casted films (equal to 50 mg of PTX) were placed to the skin's epidermal surface. A 2.5 mL sample of the media was taken at predetermined intervals. The experiment was conducted in a sink situation. Following the

proper dilution, the samples were filtered using whatman filter paper before being examined for PTX concentration using UV spectroscopy. The rate at which PTX infiltrated ($\mu\text{g}/\text{cm}^2$) the skin over time (min) was shown. The slope of the linear part of the graph was used to calculate the steady state flux " J " ($\text{mcg cm}^{-2} \text{ h}^{-1}$). Using Eq., the permeability coefficient " K_p " (cm h^{-1}) was derived.

$$K_p = J/C_0$$

Where C_0 = Concentration of drug in donor phase and J = flux

RESULT AND DISCUSSION

The objective of the present study was to manufacture PTX-loaded PVA/PVP nanofiber film using an electrospinning technique in order to improve the prolonged release profile and therapeutic effectiveness of PTX by overcoming its current drawbacks. The NF film having nano porous structure quickly absorbs moisture via tiny spaces creating a strong adhesion. Additionally, direct systemic distribution of PTX utilizing NF film helps to delay the PTX for a longer length of time by avoiding rate-limiting steps like solubility and absorption. It also avoids the first pass effect, resulting in better bioavailability and longer-lasting pharmacological impact due to the direct

discharge of the active ingredients at the site of action.

SEM of PTX loaded PVA/ PVP fibre mats

The SEM was used to verify the production of nanofibres as shown in **Figure 1**. The SEM pictures showed the development of distinct PVA/PVP nanofibres with PTX loading that ranged in size from 100 to 200 nm. Since no drug crystals or aggregates were seen in the photos, it is assumed that the drug was molecularly disseminated and encapsulated inside the electrospun fibres. In contrast, the solvent cast film that had been loaded with PTX revealed the existence of drug crystals on its surface. The change in the solvent's evaporation rate during fabrication may also be the cause of the drug aggregates' absence or presence on the surface of the fibres or films. It took very little time for the solvent to evaporate from the fibres (i.e. during their flight to the collecting device). On the other hand, the solvent evaporation from the films happened gradually. The presence of drug aggregates on the surface of the drug-loaded as cast films may be due to the solvent's slower rate of evaporation.

X-ray diffraction studies

The produced samples were subjected to X-ray diffraction analysis in order to determine if any polymorphic transitions (if any) may

have occurred in PTX when it was made into nanofibres. Furthermore, utilising the relative integrated intensity of reflection peaks in the specified range of reflecting angle 2θ , XRD patterns may be utilized to assess the degree of crystallinity of a sample. The XRD spectra of the drug PTX, PVA-PVP film and drug-loaded nanofiber patches are shown in **Figure 2**. The pure drug's XRD pattern exhibits a number of diffraction peaks demonstrating the crystal structure of PTX. The sharp peaks are seen at diffraction angles of 13.91° , 16.77° and 27.27° as shown in Fig 2C. However, PVA-PVP films have two distinct peaks at 19.37° and 29.21° for PVA and PVP respectively as depicted in **Figure 2a**. The XRD spectra of a PVA-PVP nanofiber patch with PTX loaded are shown in **Figure 2b**. It is noted that the PVA-PVP-related peaks, which arise at 19.6° and 29.4° and are pushed higher in the diffraction angle are broadened. The peaks are visible despite the drug's modest intensity level. This suggests that the medicine interacts with polymers, changing the molecule's original crystalline structure.

Differential scanning calorimetry

The findings of the XRD tests were verified by DSC thermograms of produced samples as depicted in **Figure 3**. The degree of crystallinity associated with a molecule may

be determined by measuring the temperature and energy fluctuation involved in its phase transitions using a technique called DSC. To demonstrate its crystalline nature, PTX alone displayed a pronounced endothermic peak at 105.8°C which corresponds to its melting point. The PVP K-30 and PVA both displayed a wide endotherm on the DSC thermogram at temperatures of 67.2°C and 224.3°C respectively. Furthermore, the absence of the peak linked to the melting temperature of PTX when it was formed as nanofibres indicated that it had completely amorphized. Consequently, the DSC study findings were consistent with the XRD analysis.

Fourier transforms infrared spectroscopy

The FTIR spectra was captured for PTX, PVA-PVP, PTX loaded as cast films and PTX loaded nanofibres. The PTX alone showed characteristic band at 1700 cm^{-1} (C=O & C=N stretching), $2800\text{-}2900\text{ cm}^{-1}$ (C-H stretching). The PVP showed peaks at 1691 cm^{-1} (C=O), $2800\text{-}2900$ (C-H stretching), 3098 cm^{-1} (C=C stretching) as well as PVA showed peaks at 3306 cm^{-1} (O-H stretching), 3062 cm^{-1} (C=C stretching). The PTX-PVA-PVP mat shows peaks at 1700 cm^{-1} (C=O & C=N stretching), $2800\text{-}2900\text{ cm}^{-1}$ (C-H stretching), 3098 cm^{-1} (C=C stretching). The spectra of PTX-loaded

nanofibres and of the cast film demonstrated retention of all the PTX and PVA-PVP characteristic bands. Due to the lack of any chemical interaction, there was also no significant shifting of the existing bands or the emergence of new bands that would indicate compatibility of PTX with PVA-PVP (**Figure 4**).

Drug content and encapsulation efficiency

In contrast to solvent cast films, which exhibited PTX loading of roughly $64.8 \pm 1.21\%$ w/w, produced e-spun PVP nanofibres had PTX content of $87.52 \pm 2.1\%$ w/w. Additionally, it was discovered that the EE of e-spun PVP nanofibres was $95.43 \pm 1.43\%$ w/w, while the EE of solvent cast films was around $73.5 \pm 2.67\%$ w/w. The films were cast at a higher temperature ($70 \pm 1^\circ\text{C}$) in order to thoroughly eliminate the solvent. The higher drug EE was the consequence of passive loading of PTX into the polymers and solidification of the content by the electrospinning process.

***In vitro* PTX diffusion studies**

The drug release profile of PTX loaded PVA-PVP mat and film was shown in **Figure 5**. The polymer matrix rate of deterioration and disintegration has a big impact on how quickly drugs are released. The medication-loaded water-soluble polymers that were spun into fibres and employed as quick-

release carriers for oral drug administration have been used in the past. Utilizing a water-soluble component may also help ensure that all of the active components are released completely, preventing any trapping or sluggish release of a small dose near the end of the release profile. To regulate the PTX release rate in this investigation, we combined PVA with water-soluble polyvinyl pyrrolidone (PVP). The release rate of PTX increases when PVP ratio rises. As a result of the water-soluble PVP included in the fibre matrix, holes are formed inside the fibres that allow the medicine to be released completely and continuously into the environment. The degree of swelling that the matrix material experiences in water may also regulate the medication release rate. In this situation, the pores of a hydrophilic substance open up as a result of swelling after absorbing water, making it easier for medications to diffuse out of the matrix. The comparison study between PTX loaded nanofiber mat and casting film show nanofiber will having advantage being used as sustained drug delivery.

***In vitro* release kinetics**

The drug release profile of each formulation was examined in order to determine the PTX release mechanism from the fibres by applying the Zero-order, Higuchi and Peppas

models. The measured drug release profile (at pH 6.8) suited the Higuchi model well, according to formulation ($R^2 > 0.977$ for the formulation). As a result, at pH 6.8, drug release was regulated by diffusion. This may be explained by the display which releases in bursts at first and then slowly sustains them for up to 8–9 hours. Our tests have shown that this cutting-edge medication delivery idea has a great deal of promise for treating oral submucosal fibrosis more successfully.

Ex vivo skin permeation

Since the flux of the nanofibres mats was 17 times more than that of the as cast film according to **Table 1**, the ex vivo skin permeation data showed that they were superior to as cast films. Additionally, it was discovered that nanofibres had a higher permeability coefficient than films. The

advantage of nanofibre mats over cast films can be attributed to the solubility improvement of PTX as a result of molecular dispersion within PVA-PVP, fast swelling of porous nanofibre mats due to small size and enormous increase in area, ultimately leading to leaching out of PTX molecules at a faster rate when compared to cast films. Additionally, both PTX loaded nanofibre mats and as cast PVA PVP films showed a linear rise in the permeation flux with an increase in PTX. This might be explained by a decrease in the proportion of polymer, which serves as a diffusion barrier for PTX and increases PTX release. As a result, the larger absorption of PTX from the nanofibre mats was made possible by the higher concentration gradient.

Table 1: Mucosal skin permeation kinetics of pentoxifylline from PTX loaded nanofiber mats and as cast film

Formulation	PTX loaded nanofibers	PTX loaded solvent cast films
Flux	5.01± 0.38	0.301±0.23
Permeability	0.00482	0.000588

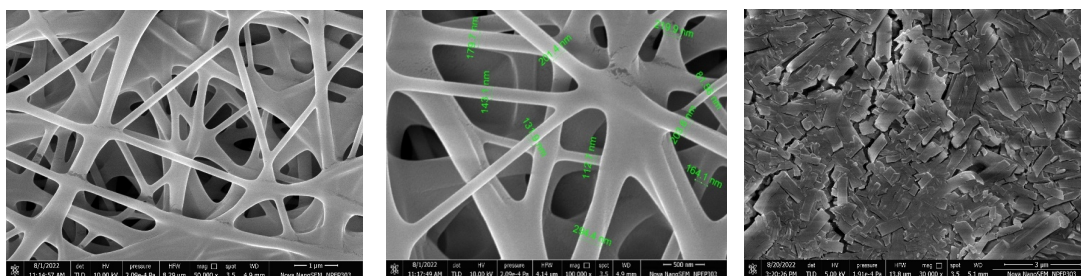


Figure 1: SEM Images of (a) PTX loaded nanofiber mat at 50,000× (b) PTX loaded nanofiber mat at 100,000× (c) PTX loaded film at 30,000×

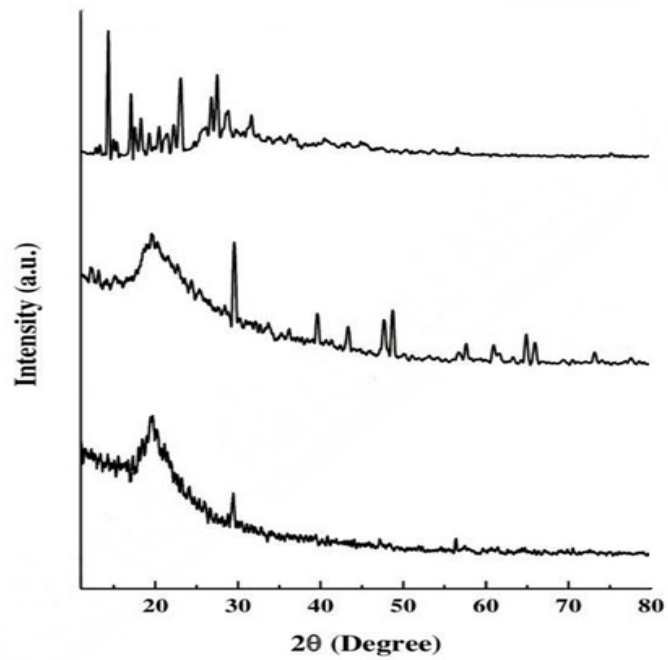


Figure 2: XRD of (a) PVA-PVP film (b) PTX loaded nanofiber mat (c) PTX Drug

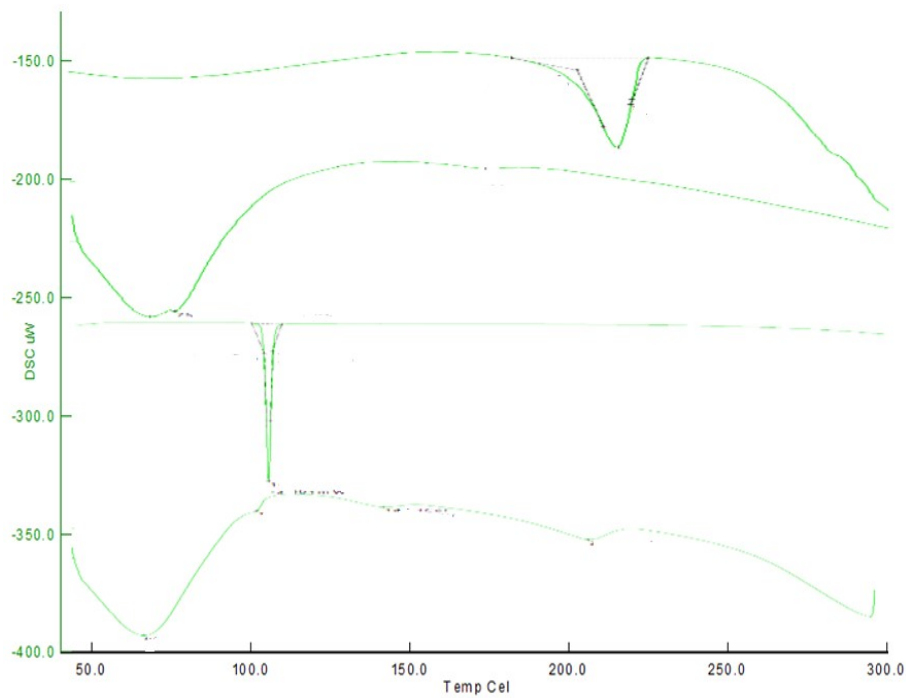


Figure 3: DSC Thermogram of (a) PVA-PVP (b) Nanofiber mat (c) PTX drug

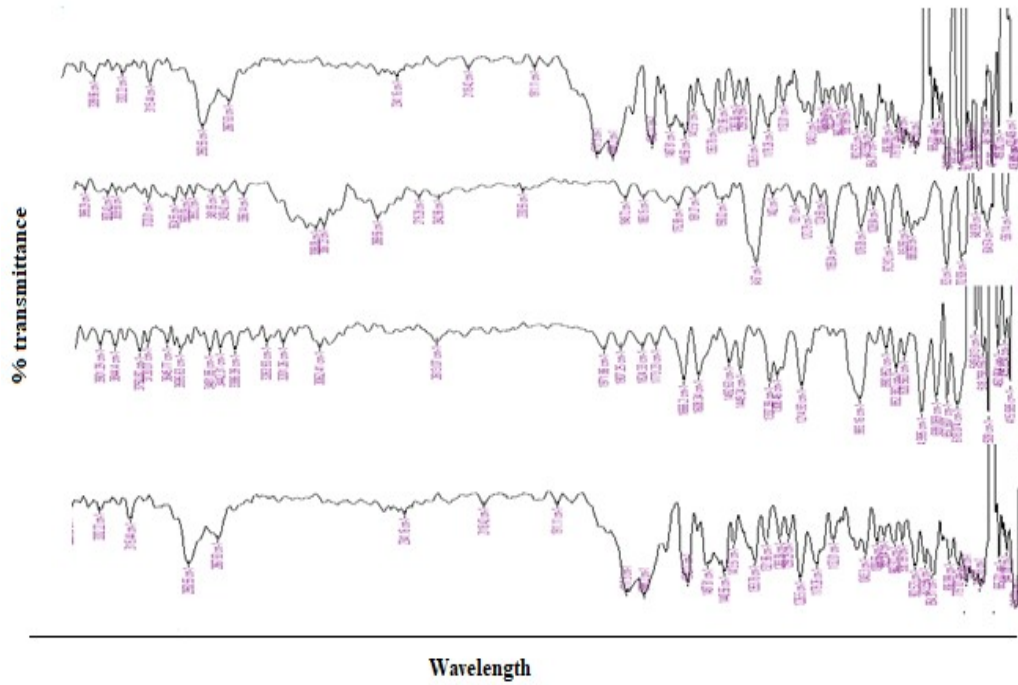


Figure 4: FTIR Spectra of PTX, PVA- PVP, PTX loaded film, PTX loaded nanofiber mat

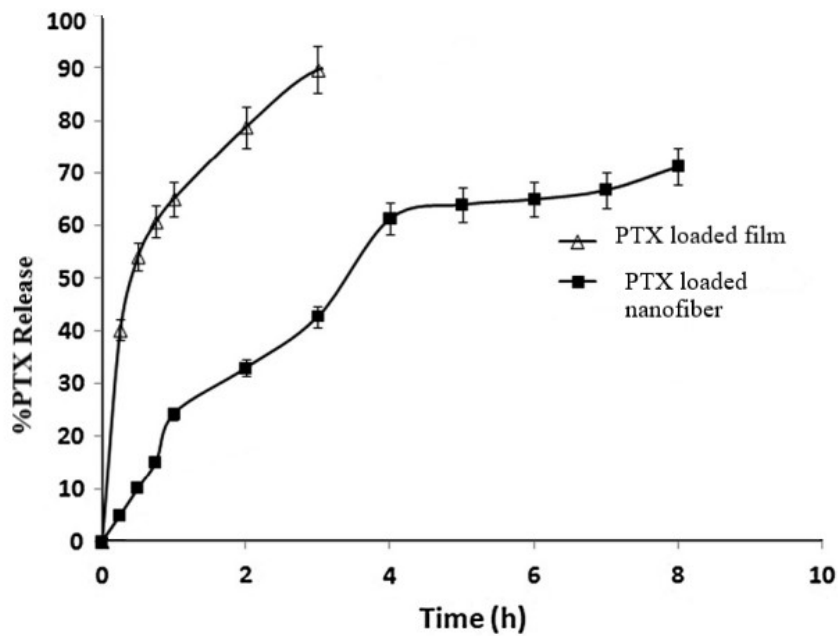


Figure 5: *In-vitro* drug diffusion of PTX loaded film and PTX loaded nanofiber mat

CONCLUSION

Using the electrospinning approach, PTX-loaded nanofibre mats were successfully created in the current study. When analysed for *in vitro* PTX release and *ex vivo* mucosal skin penetration experiments, the manufactured nanofibre mats of PTX were found to be superior to PTX supplied as cast films. The amorphization with reduced PTX particle size, PTX dispersion at the molecular level in the PVA-PVP matrix, and significantly increased area for PTX dissolution due to nanonization, as revealed by SEM, XRD, and DSC studies, could all be responsible for the improvement in drug delivery kinetics of PTX loaded nanofibre mats. In order to optimise its biopharmaceutical qualities and increase therapeutic effectiveness in oral submucosal fibrosis, mucoadhesive patch with PTX loaded nanofibres might be thought of as an alternate dosage form.

REFERENCE

- [1] Wollina U, Verma SB, Ali FM, Patil K. Oral submucous fibrosis: An update. *Clin Cosmet Investig Dermatol*. 2015 Apr 13; 8:193–204.
- [2] Rajendran R. Oral submucous fibrosis: etiology, pathogenesis, and future research. 1994.
- [3] Tilakaratne WM, Klinikowski MF, Saku T, Peters TJ, Warnakulasuriya S. Oral submucous fibrosis: Review on etiology and pathogenesis. Vol. 42, *Oral Oncology*. 2006. p. 561–8.
- [4] Yang YH, Lien YC, Ho PS, Chen CH, Chang J, Cheng TC, *et al*. The effects of chewing areca/betel quid with and without cigarette smoking on oral submucous fibrosis and oral mucosal lesions.
- [5] Sheetal S Choudhari *et al* 242 ABSTRACT.
- [6] Sarode SC, Sarode GS. Burning sensation in oral submucous fibrosis and its possible association with mucin secreted by affected minor salivary glands. *Oral Oncol*. 2013 Apr;49(4).
- [7] Aziz SR. Oral submucous fibrosis: case report and review of diagnosis and treatment. *J Oral Maxillofac Surg*. 2008 Nov;66(11):2386–9.
- [8] Arakeri G, Brennan PA. Oral submucous fibrosis: an overview of the aetiology, pathogenesis, classification, and principles of management. *British Journal of Oral and Maxillofacial Surgery*. 2013 Oct 1;51(7):587–93.

- [9] Rao NR, More CB, Brahmabhatt RM, Chen Y, Ming W kit. Causal inference and directed acyclic graph: An epidemiological concept much needed for oral submucous fibrosis. *J Oral Biol Craniofac Res.* 2020 Oct 1;10(4):356–60.
- [10] Jani Y, Chaudhary A, Dudhia B, Bhatia P, Soni N, Patel P. Evaluation of role of trace elements in oral submucous fibrosis patients: A study on Gujarati population. *J Oral Maxillofac Pathol.* 2017 Sep 1;21(3):455.
- [11] Hassan I, Dorjay K, Anwar P. Pentoxifylline and its applications in dermatology. *Indian Dermatol Online J.* 2014;5(4):510.
- [12] Magnusson M, Gunnarsson M, Berntorp E, Björkman S, Höglund P. Effects of pentoxifylline and its metabolites on platelet aggregation in whole blood from healthy humans. *Eur J Pharmacol.* 2008 Mar 10;581(3):290–5.
- [13] Zhou QG, Zheng FL, Hou FF. Inhibition of tubulointerstitial fibrosis by pentoxifylline is associated with improvement of vascular endothelial growth factor expression. *Acta Pharmacologica Sinica* 2009 30:1. 2008 Dec 15;30(1):98–106.
- [14] Zhou QG, Zheng FL, Hou FF. Inhibition of tubulointerstitial fibrosis by pentoxifylline is associated with improvement of vascular endothelial growth factor expression. *Acta Pharmacologica Sinica* 2009 30:1. 2008 Dec 15;30(1):98–106.
- [15] Mahajan AD, Tatu RJ, Shenoy NA, Sharma VS. Surgical management of oral submucous fibrosis in an edentulous patient: A procedural challenge. *Natl J Maxillofac Surg.* 2010;1(2):161.
- [16] Al Shuwaili AH, Rasool BKA, Abdulrasool AA. Optimization of elastic transfersomes formulations for transdermal delivery of pentoxifylline. *Eur J Pharm Biopharm.* 2016 May 1;102:101–14.
- [17] Liska DA, Akucewich LH, Marsella R, Maxwell LK, Barbara JE, Cole CA. Pharmacokinetics of pentoxifylline and its 5-hydroxyhexyl metabolite after oral and intravenous administration of pentoxifylline to healthy adult horses. *Am J Vet Res.* 2006 Sep;67(9):1621–7.

- [18] George J, Abel P. Pentoxifylline. *xPharm: The Comprehensive Pharmacology Reference*. 2022 May 29;1–18.
- [19] Shailendrakumar AM, Ghate VM, Kinra M, Lewis SA. Improved Oral Pharmacokinetics of Pentoxifylline with Palm Oil and Capmul® MCM Containing Self-Nano-Emulsifying Drug Delivery System. *AAPS PharmSciTech*. 2020 May 1;21(4).
- [20] Abasalta M, Asefnejad A, Khorasani MT, Saadatabadi AR. Fabrication of carboxymethyl chitosan/poly(ϵ -caprolactone)/doxorubicin/nickel ferrite core-shell fibers for controlled release of doxorubicin against breast cancer. *Carbohydr Polym*. 2021 Apr 1;257:117631.
- [21] Wade SJ, Zuzic A, Foroughi J, Talebian S, Aghmesheh M, Moulton SE, *et al*. Preparation and in vitro assessment of wet-spun gemcitabine-loaded polymeric fibers: Towards localized drug delivery for the treatment of pancreatic cancer. *Pancreatology*. 2017 Sep 1;17(5):795–804.
- [22] Abid S, Hussain T, Raza ZA, Nazir A. Current applications of electrospun polymeric nanofibers in cancer therapy. *Materials Science and Engineering: C*. 2019 Apr 1;97:966–77.
- [23] Chan Z, Chen Z, Zhang A, Hu J, Wang X, Yang Z. Electrospun nanofibers for cancer diagnosis and therapy. *Biomater Sci*. 2016 May 24;4(6):922–32.
- [24] Bhardwaj N, Kundu SC. Electrospinning: A fascinating fiber fabrication technique. *Biotechnol Adv*. 2010 May 1;28(3):325–47.
- [25] Moradkhannejhad L, Abdouss M, Nikfarjam N, Shahriari MH, Heidary V. The effect of molecular weight and content of PEG on in vitro drug release of electrospun curcumin loaded PLA/PEG nanofibers. *J Drug Deliv Sci Technol*. 2020 Apr 1;56:101554.
- [26] Samadzadeh S, Mousazadeh H, Ghareghomi S, Dadashpour M, Babazadeh M, Zarghami N. In vitro anticancer efficacy of Metformin-loaded PLGA nanofibers towards the post-surgical therapy of lung cancer. *J Drug Deliv Sci Technol*. 2021 Feb 1;61:102318.
- [27] Hu X, Li J, Chen Q, Lin Z, Yin D. Combined effects of aqueous

- suspensions of fullerene and humic acid on the availability of polycyclic aromatic hydrocarbons: Evaluated with negligible depletion solid-phase microextraction. *Science of The Total Environment*. 2014 Sep 15;493:12–21.
- [28] Palmer LC, Stupp SI. Molecular self-assembly into one-dimensional nanostructures. *Acc Chem Res*. 2008 Dec 16;41(12):1674–84.
- [29] Luo CJ, Stoyanov SD, Stride E, Pelan E, Edirisinghe M. Electrospinning versus fibre production methods: from specifics to technological convergence. *Chem Soc Rev*. 2012 Jun 13;41(13):4708–35.
- [30] Sun B, Long YZ, Zhang HD, Li MM, Duvail JL, Jiang XY, *et al*. Advances in three-dimensional nanofibrous macrostructures via electrospinning. *Prog Polym Sci*. 2014 May 1;39(5):862–90.
- [31] Wang M, Hou J, Yu DG, Li S, Zhu J, Chen Z. Electrospun tri-layer nanodepots for sustained release of acyclovir. *J Alloys Compd*. 2020 Dec 15;846:156471.
- [32] Ding Y, Dou C, Chang S, Xie Z, Yu DG, Liu Y, *et al*. Core-Shell Eudragit S100 Nanofibers Prepared via Triaxial Electrospinning to Provide a Colon-Targeted Extended Drug Release. *Polymers* 2020, Vol 12, Page 2034. 2020 Sep 7;12(9):2034.
- [33] Zhao K, Kang SX, Yang YY, Yu DG. Electrospun Functional Nanofiber Membrane for Antibiotic Removal in Water: Review. *Polymers* 2021, Vol 13, Page 226. 2021 Jan 11; 13(2):226.
- [34] Kazsoki A, Farkas A, Balogh-Weiser D, Mancuso E, Sharma PK, Lamprou DA, *et al*. Novel combination of non-invasive morphological and solid-state characterisation of drug-loaded core-shell electrospun fibres. *Int J Pharm*. 2020 Sep 25;587:119706.
- [35] Patil S, Choudhary B, Rathore A, Roy K, Mahadik K. Enhanced oral bioavailability and anticancer activity of novel curcumin loaded mixed micelles in human lung cancer cells. *Phytomedicine*. 2015 Nov 15;22(12):1103–11.
- [36] (PDF) Comparative Studies of Pentoxifylline -Active Substance and Tablets [Internet]. [cited 2022 Oct 17]. Available from:

https://www.researchgate.net/publication/282914342_Comparative_Studies_of_Pentoxifylline_Active_Substance_and_Tablets

- [37] Bartosova L, Bajgar J. Transdermal Drug Delivery In Vitro Using Diffusion Cells. *Curr Med Chem.* 2012 Oct 11; 19(27):4671–7.